Bioorganic Chemistry 108 (2021) 104686

Contents lists available at ScienceDirect

Bioorganic Chemistry

journal homepage: www.elsevier.com/locate/bioorg

Synthesis of imidazole-pyrazole conjugates bearing aryl spacer and exploring their enzyme inhibition potentials

Faryal Chaudhry [a,b,*], Wardah Shahid [c], Mariya al-Rashida [d], Muhammad Ashraf [c], Munawar Ali Munawar [a,*], Misbahul Ain Khan [a,c]

[a] Institute of the Chemistry, Quaid-e-Azam Campus, University of the Punjab, Lahore 54590, Pakistan
[b] Department of Chemistry, Kinnaird College for Women Lahore, 93-Jail Road, Lahore 54000, Pakistan
[c] Department of Chemistry, The Islamia University of Bahawalpur, Bahawalpur 63100, Pakistan
[d] Department of Chemistry, Forman Christian College (A Chartered University), Ferozepur Road, Lahore 54600, Pakistan

ARTICLE INFO

Keywords:
α-Glucosidase
Imidazole
Lipoxygenase
Molecular Docking
Pyrazole

ABSTRACT

Developing improved enzyme inhibitors is an effective therapy to counter various diseases. Aiming to build up biologically active templates, a new series of bis-diazoles conjugated with an aryl linker was designed and prepared through a convenient synthetic approach. Synthesized derivatives **6(a-m)**, having different substitutions at the 2nd position of the imidazole nucleus, depict the scope of present study. These compounds were characterized through spectroscopic methods and further examined for their *in vitro* enzyme inhibitory potentials against two selected enzymes: α-glucosidase and lipoxygenase (LOX). Overall, this series was found to be effective against α-glucosidase and moderately active against LOX enzyme. Compound **6k** was the most potent α-glucosidase inhibitor with $IC_{50} = 54.25 \pm 0.67$ μM as compared to reference drug acarbose ($IC_{50} = 375.82 \pm 1.76$ μM). The docked conformation revealed the involvement of substituent's heteroatoms with amino acid residue Gly280 through hydrogen bonding. The most active LOX inhibitor was **6a** with $IC_{50} = 41.75 \pm 0.04$ μM as compared to standard baicalein ($IC_{50} = 22.4 \pm 1.3$ μM). Docking model of **6a** suggested the strong interaction of imidazole's nitrogen with iron atom of the active pocket of enzyme. Other features like lipophilicity, bulkiness of compounds, pi-pi interactions and/or pi-alkyl interactions also affected the inhibiting potentials of all prepared scaffolds.

1. Introduction

In recent years, diazolic core has attracted attention of synthetic chemists because of its manifold applications. Among diazolic analogues; pyrazole and imidazole have constituted structural make up of natural products [1], photochromic compounds [2], frame works having optical properties [3], agrochemicals [4] and also displayed excellent catalytic potentials [5]. Heravi and Zadsirjan recently reviewed some leading drugs where such nitrogen based heterocyles were considered as the foundation of many marketed medicines such as ondansetron, losartan, apixaban, celecoxib and sildenafil [6]. These nitrogen containing motifs facilitate in pharmaceutics as anti-inflammatory [7], anticancer [8], antimicrobial [9], antidiabetic [10], antioxidant agents [11].

Enzymes are often highlighted by experimental evidences as the validated potential drug targets. In the past few decades, enzyme inhibitors have become of special interest in drug design and discovery [12]. Diazoles are privileged pharmacophores for the development of new enzyme inhibitors because of their tendency to form hydrogen bonds. Some exclusive templates of pyrazole and/or imidazole moieties have recently been designed to target enzymes like mushroom tyrosinase [13], α-amylase [14], carbonic anhydrase [15], DNA gyrase [16], nucleotide pyrophosphatase [17], cyclooxygenase [18] to cope with different diseases. One such identified target is α-glucosidase which plays a significant role in controlling a well known metabolic disease: diabetes mellitus type 2. The dilemma of this disease is that it may cause several other complications in body such as heart disease and kidney failure. Various research reports have emphasized that postprandial glucose regulation can control diabetes and inhibition of α-glucosidase is one of the useful therapies. Recently, different heterocycles have been documented as excellent α-glucosidase inhibitors that may lead to

* Corresponding authors at: Institute of the Chemistry, Quaid-e-Azam Campus, University of the Punjab, Lahore 54590, Pakistan (F. Chaudhry; M.A. Munawar); Department of Chemistry, Kinnaird College for Women Lahore, 93-Jail Road, Lahore 54000, Pakistan (F. Chaudhry).

E-mail addresses: faryal.chaudhry@kinnaird.edu.pk, frylchaudhry@yahoo.com (F. Chaudhry), mamunawar.chem@pu.edu.pk (M. Ali Munawar).

https://doi.org/10.1016/j.bioorg.2021.104686
Received 26 October 2020; Received in revised form 10 January 2021; Accepted 22 January 2021
Available online 3 February 2021

clinical trials [19–21].

A non-heme iron-containing class of metalloenzymes is lipoxygenase (LOX) that can be isolated from plants and animals. LOXs isoenzymes (most commonly 5-LOX, 12-LOX and 15-LOX) differ in their substrate specificity and mode of interaction at their binding sites. This class of enzymes exhibits multi-faceted biological functions such as production of biological mediators in signaling pathways and mobilization of lipids by oxidizing esters etc. LOX isoforms catalyze the peroxidation of arachidonic and linoleic acids to generate hydroperoxy fatty acids which further metabolize and produce lipoxins and leukotrienes. Scientists have established claims that LOX metabolites promote different human diseases such as initiation and/or progression of inflammation, atherosclerosis, oxidative stress in Alzheimer's patients, diabetes, cardiovascular diseases and development of different forms of cancer. Therefore, LOXs have been hypothesized as important therapeutic targets for both redox and non-redox inhibiting agents [22–26]. In this respect, different natural and synthetic pharmacophores have been documented [27–29]. Some pyrazole and imidazole engineered α-glucosidase and LOXs inhibiting agents have been reported as promising drug candidates [30–34]. Recently, Cornec's group identified substituted imidazoles as potential inhibiting agents of LOX pathways to deal with neurodegenerative diseases [35]. Similarly, purine-pyrazole incorporated hybrids are reported as potent LOX inhibitors with anticancer potentials [36].

To meet the requirement of effective novel enzyme inhibitors, we have been involved in designing different combinations of heterocyclic compounds [37–42]. Herein, an aryl linker is used to connect both diazolic moieties (pyrazole and imidazole) in one molecular template **6** (**a-m**) (Fig. 1). These compounds were later screened out against two enzymes (α-glucosidase and LOX) to evaluate the enzyme inhibition potentials of this new class of compounds and results were compared with standard drugs. To the best of our knowledge, this structural framework is not explored yet.

2. Results and discussion

2.1. Chemistry

Previously, we have synthesized directly linked imidazole-pyrazole, imidazole-indole and pyrazole-pyridazine hybrids which were found to be good enzyme inhibitors [37–41]. Literature reveals the significant role of spacers in enhancing the bioactivity of molecules [43]. Thus, a series of arylidenes was designed before and those products exhibited encouraging results [42]. In continuation, present project was designed where a benzene spacer is used between pyrazole and imidazole rings and to study the enzyme inhibition potencies of this linking pattern.

Initially, precursor **2** was prepared by following the reported protocols [44]. Further, a convenient one pot multi-component approach was adopted to react substrate **2** with substituted aldehdyes **3**(**a-m**), benzil (**4**) and ammonium acetate (**5**). After purifying through column chromatography, products **6**(**a-m**) were subjected to NMR studies to identify their structures and purity. Moreover, elemental analyses results also validated our findings. The scope of the present study is depicted in structural diversity generated by the modifications in R^1 with different substitutions. All products **6**(**a-m**) were obtained in good yields (Scheme 1).

To illustrate general signals of ^{1}H NMRs, a magnified view of ^{1}H NMR of **6a** is given in Fig. 2 where methyl protons appeared as two singlets. The methyl protons, present at the 3rd position of pyrazole, were spotted at δ 2.27 ppm whereas methyl group present at the 5th position of pyrazole ring appeared little upfield at δ 2.26 ppm. The signal for H-4 of pyrazole ring was found at δ 5.99 ppm as singlet. The benzene linker has two characteristic doublets with J value of 8.5 Hz. The aryl protons nearest to pyrazole appeared upfield at δ 7.10 ppm and the other two protons, adjacent to imidazole ring appeared at δ 7.35 ppm. Other compounds **6**(**b-m**) also showed the similar spectral patterns. Beside these distinguishing signals, presence of substituents was also confirmed from respective spectra. The ^{13}C NMRs possessed all characteristic signals as well. The most prominent signals were of: two methyl carbons around δ 112 ppm and δ 113 ppm, CH-4 of pyrazole in between δ

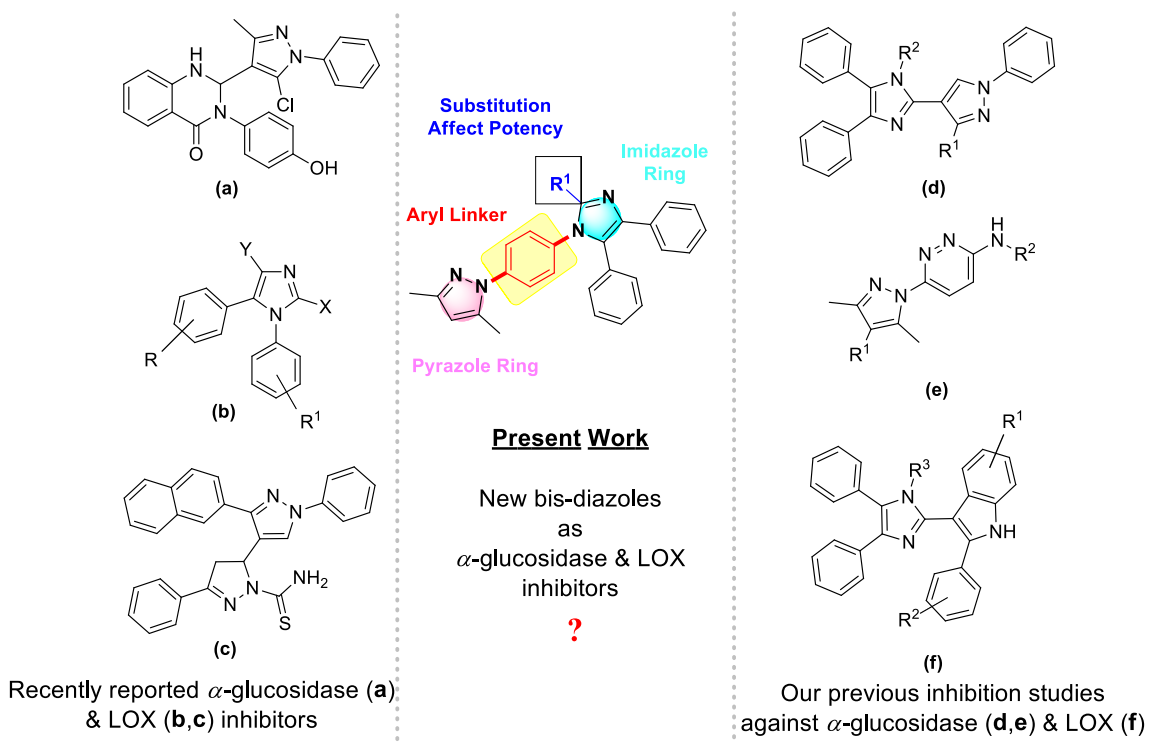

Fig. 1. Rationale of current research plan.

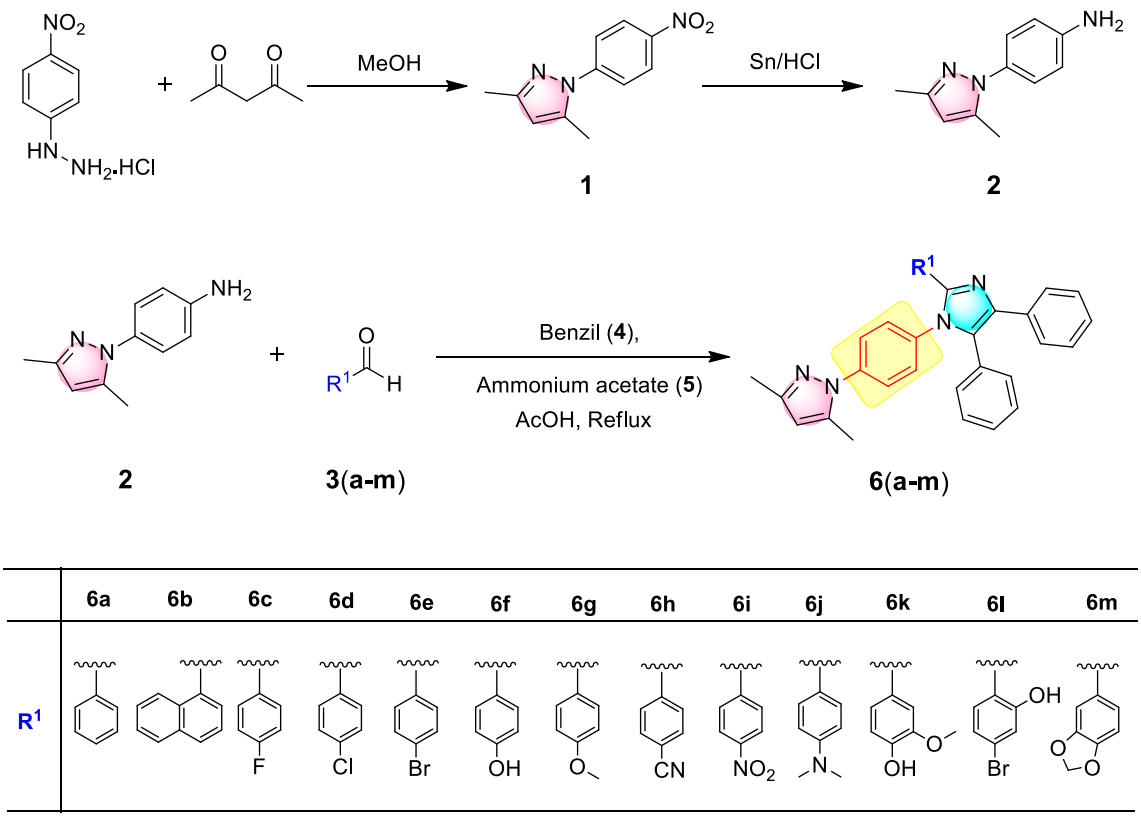

Scheme 1. Synthetic approach towards new series of imidazole-pyrazole hybrids.

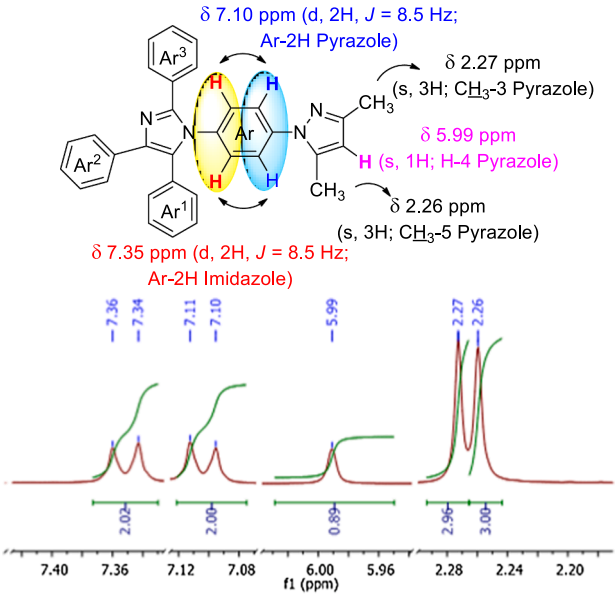

Fig. 2. Important signals in ^{1}H NMR spectrum of compound **6a**.

107–109 ppm whereas C-2 of imidazole ring appeared downfield around δ 140 ppm.

These aryl decorated scaffolds were quite stabilized; therefore, molecular ion peaks were spotted in mass spectra of all compounds. As an example of fragmentation pattern; Fig. 3 is signifying key fragmentations observed in EI-MS spectrum of **6j**. Most probably, loss of CH_3 radical, PhCN, CH_3CN and $NH(CH_3)_2$ molecules have been involved. The skeletal rearrangement (SR) of fragment *m/z* 192 lead to two interesting ions; at *m/z* 190 and *m/z* 165 [45] and these fragments were observed in each compound of this series **6(a-m)**. The experimentally found CHN percentages were also promising when compared with the calculated ones.

2.2. Biological activities

2.2.1. In vitro enzymes inhibition studies

Channar *et al.* have explored enzyme inhibitory potentials of some related 3,5-dimethylpyrazoles and investigated the effects of different substituents in the *N*-phenyl ring of pyrazole nucleus over their enzyme inhibition strengths [46]. Herein, we have prepared a comparable series of novel substituted imidazole-pyrazole hybrids **6(a-m)** which after structure elucidation was tested for their α-glucosidase and LOX inhibition potencies (Table 1). In search of potent enzyme inhibitors, we have investigated the effect of different substitutions at the 2nd position of imidazole moiety on the inhibiting efficiencies of synthesized molecules. For this purpose, α-glucosidase (from *Saccharomyces cerevisiae*) and LOX (from *Glycine* max) enzymes were selected for current enzyme inhibition studies. Acarbose was used as the standard drug for α-glucosidase inhibition which displayed activity with IC_{50} 375.82 ± 1.76 μM. Meanwhile, baicalein (with IC_{50} 22.4 ± 1.3 μM) was used as standard inhibitor for LOX inhibition study.

2.2.2. Inhibition of α-Glucosidase

Inhibition of α-glucosidase enzyme is one of the useful methods to reduce post-prandial increase in blood glucose level of diabetic patients. Azimi's research group has recently proposed few pyrazole core based molecules as significant α-glucosidase inhibitors [47]. Herein, structural variety (at the Ar^3 ring) of synthesized series and the inhibition results of products helped us to identify the general features that probably control inhibiting potencies of these compounds. Overall compounds have displayed moderate to excellent inhibition data (Fig. 4). By comparing the results of **6a** and **6b**, the compound **6a** with IC_{50} 105.17 ± 0.94 μM has exhibited better inhibition potential than of **6b** with IC_{50} 213.32 ± 1.38

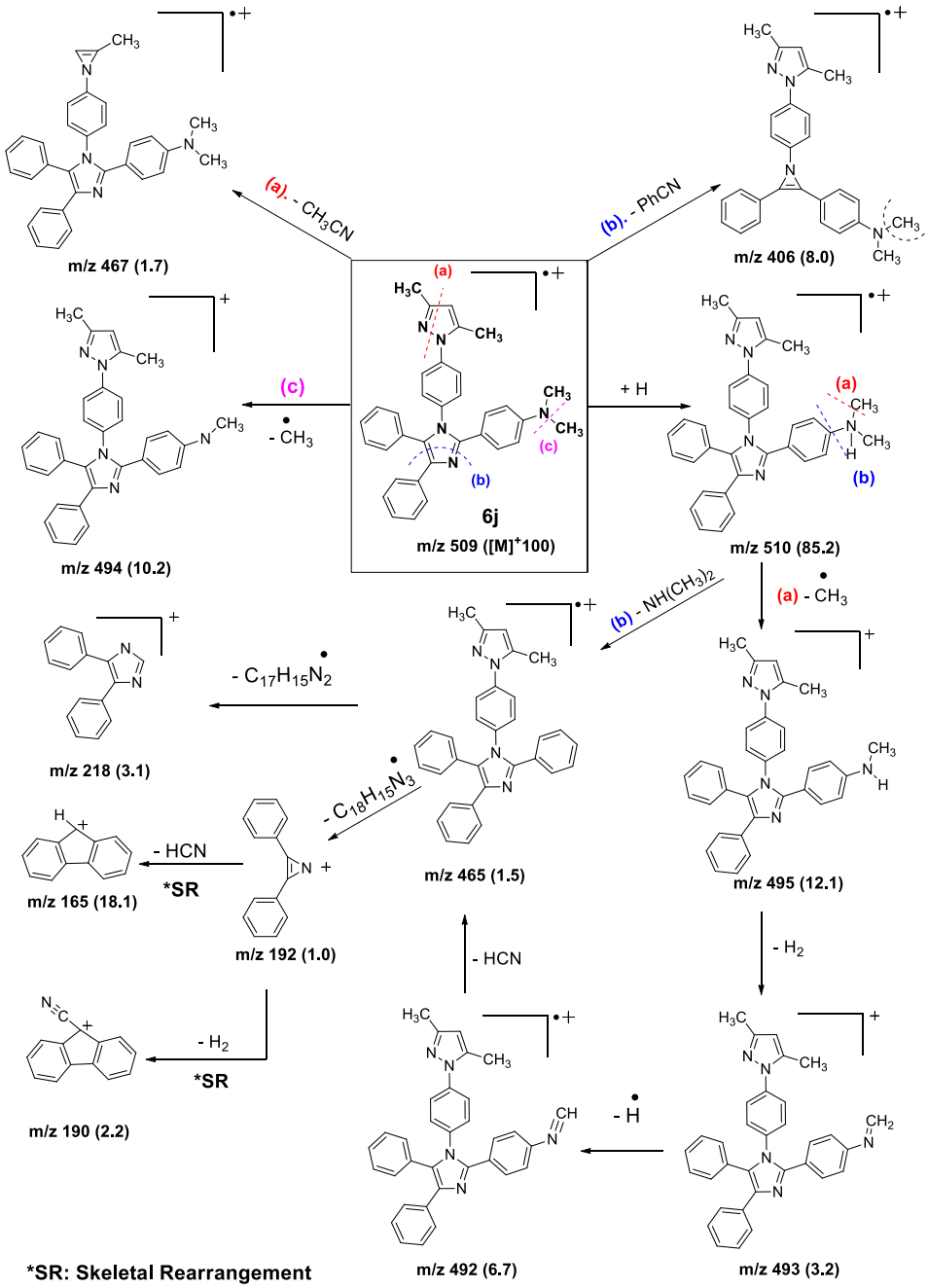

Fig. 3. Plausible EI-MS fragmentation pattern of compound **6j**.

μM. Perhaps, transferring to bulky naphthyl group has reduced the activity. The derivatives **6c**, **6d** and **6e**, substituted with the moderate halogen atoms, also found to be good inhibitors. Among these, fluoro substituted **6c** (IC_{50} 179.61 ± 1.31 μM) executed the best results amongst **6c**, **6d** and **6e**.

Further, the *para*-hydroxyl (**6f**) and *para*-methoxy (**6g**) groups containing compounds displayed good inhibition profiles with IC_{50} 224.91 ± 1.56 μM and IC_{50} 379.51 ± 2.54 μM, respectively. It has been proposed that the presence of both hydroxyl and methoxyl groups are possibly involved in hydrogen bonding with the active site of the enzyme and thus improving the inhibiting potential. By looking at the structural features of the most potent agent **6k** (IC_{50} 54.25 ± 0.67 μM), the presence of *para*-hydroxyl and *meta*-methoxyl groups in ring Ar^3 are seemed to be synergistically engaged in substantially enhancing the activity. Conversely, the shifting of hydroxyl group to ortho position, as in analog **6l**, there was marked decline in the activity. It is the most probable; the hydroxyl group is involved in intramolecular hydrogen bonding thus reducing the inhibiting potency. The presence of electron withdrawing group, such as nitro, usually improves the activity [47]. In present series, however, substitution of nitrile **6g** or nitro **6h** groups at the *para* position of Ar^3 ring reduced the activity. Compound **6m** has shown better results because of the presence of 1,3-benzodioxole moiety.

2.2.3. Inhibition of LOX

We explored the LOX inhibition of indole-imidazole hybrids previously [37]. In the present study, we aimed to engineer novel hetaryl conjugates with different substituents to observe the effects of such structural variations on the bioactivity. Towards this aim, compound **6a** was tested first and showed the best results with IC_{50} 41.75 ± 0.04 μM.

Table 1
α-Glucosidase (**6a**, **6k**) and LOX inhibition activities of diazolic conjugates **6(a-m)**.

Compound	α-Glucosidase		LOX	
	Inhibition (%) at 0.5 mM	IC_{50} (μM)	Inhibition (%) at 0.25 mM	IC_{50} (μM)
6a	98.54 ± 1.93	105.17 ± 0.94	99.61 ± 0.93	41.75 ± 0.04
6b	88.94 ± 2.45	213.32 ± 1.38	94.91 ± 1.14	52.82 ± 0.03
6c	98.78 ± 2.78	179.61 ± 1.31	68.28 ± 1.08	121.35 ± 0.96
6d	98.76 ± 1.87	184.61 ± 0.95	91.86 ± 1.87	132.25 ± 1.08
6e	98.19 ± 1.87	194.81 ± 1.29	78.89 ± 1.05	153.28 ± 0.93
6f	82.84 ± 2.37	224.91 ± 1.56	28.81 ± 1.11	NA
6g	94.66 ± 1.53	379.51 ± 2.54	82.82 ± 1.21	239.36 ± 0.96
6h	11.76 ± 2.11	NA	26.41 ± 1.12	NA
6i	97.19 ± 2.35	245.33 ± 1.75	55.34 ± 1.41	245.86 ± 1.12
6j	91.73 ± 1.32	203.54 ± 2.11	67.89 ± 1.05	75.23 ± 0.03
6k	97.89 ± 1.54	54.25 ± 0.67	75.58 ± 1.63	61.97 ± 1.15
6l	35.57 ± 2.22	NA	26.31 ± 1.08	NA
6m	95.94 ± 2.13	182.73 ± 1.19	97.13 ± 0.87	53.36 ± 0.02
Acarbose[a]	65.73 ± 1.93	375.82 ± 1.76	–	–
Baicalein[b]	–	–	93.79 ± 1.27	22.4 ± 1.3

[c]NA: Not active.
[a] Acarbose (0.5 mM) used as positive control for α-glucosidase inhibition.
[b] Baicalein (0.25 mM) used as positive control for LOX inhibition.

Efforts were made to introduce further structural modifications in Ar^3 ring with different functionalities. Extending the phenyl to naphthyl group (compound **6b**) has also displayed better results (IC_{50} 52.82 ± 0.03). Apparently, the presence of phenyl rings was more favorable for enzyme inhibition. In literature, some dihydropyrazoles were screened for LOX inhibition activity. The chloro and *para*-tolyl analogues were the most active [48]. However, substitutions of halogens in Ar^3 ring were not much effective for us to reduce the enzyme activities. Hence, compounds **6c**, **6d**, and **6e** have exhibited moderate inhibition. As a next step, replacement with electron rich or poor groups **6(f-i)** did not improve their potencies either. However, **6j** with -$N(CH_3)_2$ substitution improved its activity to (IC_{50} 75.23 ± 0.03). To further explore, the presence of methoxyl group at the meta position and hydroxyl at the para position of Ar^3 in compound **6k** apparently enhanced the activity to IC_{50} 61.97 ± 1.15, though, **6l** was found to be inactive. Another derivative **6m** has also displayed excellent inhibition profiles (IC_{50} 53.36 ± 0.02) which partially can be justified that possibly the oxygen atoms are participating to make additional H-bonds with amino acid residues of enzyme. Overall, results signify compound **5a** to be the most potent inhibitor of the series (Fig. 4). Docking of lead inhibitors further explained the observed relationships.

2.3. Molecular docking studies

2.3.1. Docking of α-Glucosidase inhibitors

For α-glucosidase docking studies, two of the most active inhibitors **6k** (IC_{50} = 54.25 ± 0.67 μM) and **6a** (IC_{50} = 105.17 ± 0.94 μM) were selected. A number of non-bonded interactions were observed (Table 2). Compound **6a** was the second most active inhibitor, its docked conformation and binding site interactions are shown in Fig. 5.

In accordance to the literature, nitrogen atoms have usually made hydrogen bonds at the enzyme's binding sites to make ligand fitted well in the cavity [47,49]. Here it was observed that one of the nitrogen atoms of the imidazole ring was making a hydrogen bond with Asn246, while one of the nitrogen atoms of the pyrazole ring was making a hydrogen bond with Gly280. One of the phenyl rings attached to the imidazole ring was making a pi-pi *T*-shaped interaction with Trp242. The phenyl ring, attached to the nitrogen atom of the imidazole ring was making a pi-pi stacked interaction with His245. Fig. 5 also shows docked conformation of most active inhibitor **6k**. Apparently, the change in observed potency was due to different snug fit orientation. The amino acid Gly280 was acting as a hydrogen bond donor (towards the oxygen atom of the methoxy group), and as a hydrogen bond acceptor (towards the hydroxyl group). One of the phenyl groups attached to the imidazole ring was making a pi-alkyl interaction with Pro309. The pyrazole ring was also making a pi-alkyl interaction with Ala326.

2.3.2. Docking of LOX inhibitors

Compound **6a** was the most active LOX inhibitor (IC_{50} = 41.75 ± 0.04 μM), closely followed by compounds **6b** and **6m** (having almost same inhibition activities, IC_{50} = 52.82 ± 0.03, and 53.36 ± 0.02 μM, respectively). Hence, these compounds were selected for the docking studies. The enzyme crystal structure was downloaded from the PDB (PDB ID: 3V99). Fig. 6 shows docked conformation of **6a**. For this compound, no hydrogen bonded interactions were observed; instead, two of the most important interactions observed were hydrophobic interactions and the interaction of the imidazole nitrogen with the Fe atom of the enzyme's active site.

Among hydrophobic interactions, the pi-alkyl interactions between Leu368 and the phenyl group attached to the imidazole ring. Gedawy *et al.* have proposed comparable hydrophobic interactions between Leu368 and aryl ring of pyrazole sulfonamides [50]. Other observed interactions were among phenyl ring (also substituted on imidazole ring) and Ala672, and between Ala410 and the phenyl ring attached to the nitrogen atom of the imidazole ring. Ala410 was also making a pi-alkyl interaction with the pyrazole ring, as well as making hydrophobic interactions with the methyl groups attached to the pyrazole ring.

Compounds **6b** and **6m** showed almost similar inhibition patterns with different binding modes. The docked conformations and binding site interactions of **6b** revealed that the nitrogen atom of the imidazole ring was making a hydrogen bond with Phe177. A number of pi-alkyl interactions were observed, one of the phenyl rings attached to the imidazole ring was making a pi-alkyl interaction with Ala410, while the two methyl groups attached to the pyrazole ring were also making pi-alkyl interactions with Leu607 and Ala672. For compound **6m**, two oxygen atoms of the benzodioxole ring were hydrogen bonded with Asn554 and Gln557. Again hydrophobic interactions were observed to be of importance in imparting stability to the enzyme-inhibitor complex. Ala410 was making a pi-sigma and a pi-alkyl interaction with two phenyl rings attached to the imidazole ring. Another pi-sigma interaction was observed between Leu607 and the remaining phenyl group attached to the imidazole ring. Leu607 was also making a pi-alkyl interaction with the pyrazole ring, while one of the methyl groups attached to the pyrazole ring. Overall results are in agreement with the documented reports where methyl groups gave flexibility in bond rotation, heteroatoms formed hydrogen bonds to give stability and the heterocyclic/aromatic pi-rings involved in aromatic interactions [47–50].

3. Conclusion

In conclusion, a novel series of phenyl bridged imidazole-pyrazole scaffolds **6(a-m)** was designed and synthesized. Unlike our previous findings where anilines were used to produce varied *N*-substitutions in imidazole ring, herein, a variety of substituted aldehydes were exploited to investigate the enzyme inhibitory effects of different substitutions at the 2nd position of imidazole ring. The chemical structures were proposed on the basis of observed spectral data. Later, these compounds

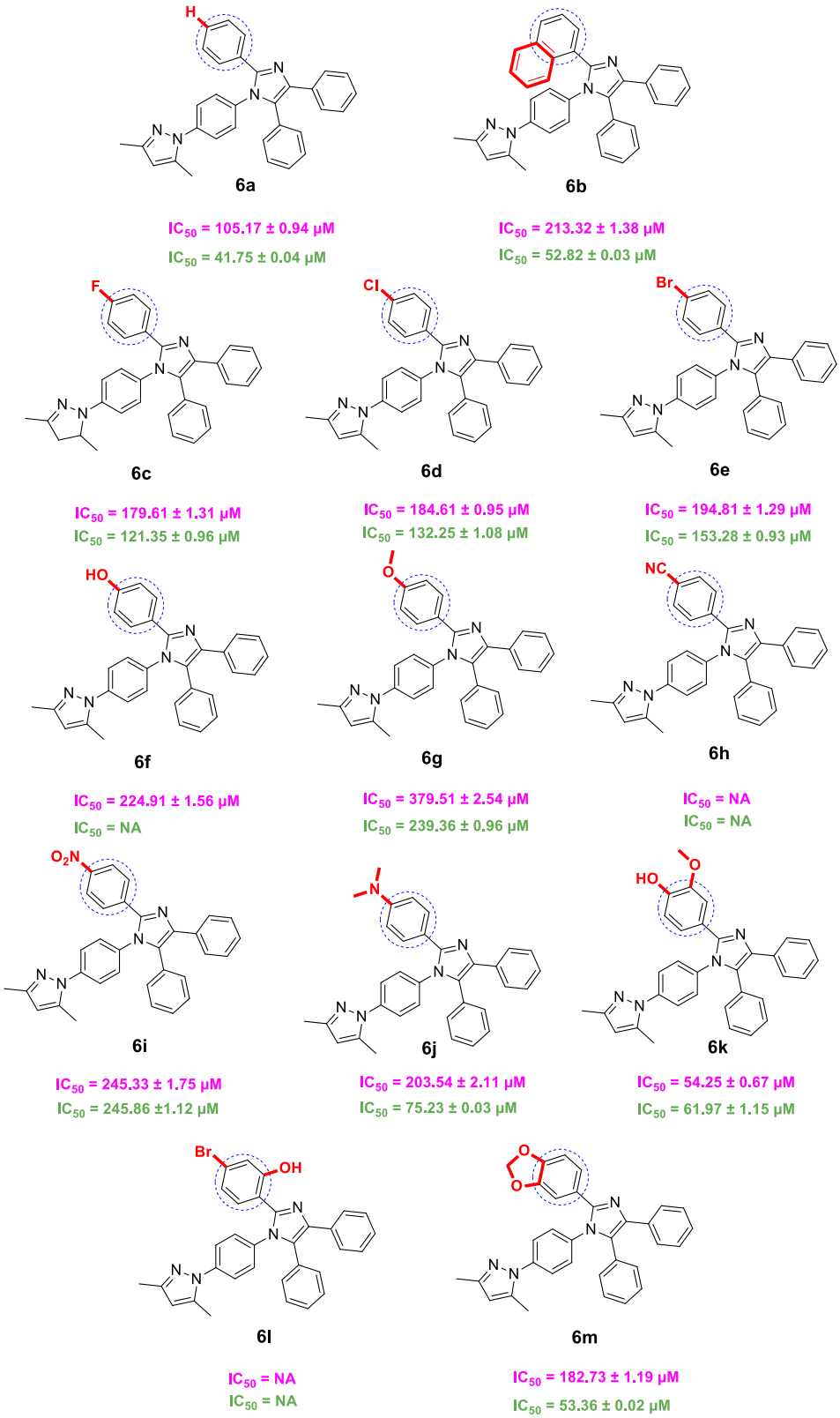

Fig. 4. Comparative enzyme inhibition potentials of compounds **6(a-m)** against α-glucosidase (IC_{50} values in pink) and LOX (IC_{50} values in green). (For interpretation of the references to colour in this figure legend, the reader is referred to the web version of this article.)

were tested for their enzyme inhibition potentials. Preliminary screening studies were carried out against α-glucosidase and LOX enzymes. Overall decreasing order of α-glucosidase inhibition was: **6k** > **6a** > **6c** > **6m** > **6d** > **6e** > **6j** > **6b** > **6f** > **6i** > acarbose > **6g** > **6l** > **6h**. These results suggest that modifications in Ar^3 ring most probably affected the enzyme activity. However, this series displayed moderate inhibitory effects against LOX enzyme with IC_{50} between 41.75 and 245.86 μM. Compounds **6a**, **6b** and **6m** can be considered as good lead

Table 2
Binding free energies and non-bonded interactions of α-glucosidase inhibitors (**6a**, **6k**) and LOX inhibitors (**6a**, **6b**, **6m**) with their respective receptors.

Ligand	Binding free energy (kJ/mol)	Hydrophobic interactions	Hydrogen bond interactions	Hydrogen bond distance (Å)	Other interactions and distance (Å)
α-Glucosidase Inhibitors					
6a	−13	His245 (pi-pi stacked), Trp242 (pi-pi *T*-shaped)	Asn246, Gly280	1.74, 2.33	_
6k	−29	Pro306 (pi-alkyl), Ala326 (pi-alkyl)	Gly280 (H-bond acceptor), Gly280 (H-bond donor)	1.73, 1.83	_
LOX Inhibitors					
6a	−25	Ala410 (alkyl and pi-alkyl), Ala672 (pi-alkyl), Leu368 (pi-alkyl)	_	_	Lig-Fe^{2+} (2.22)
6b	−23	Leu607 (alkyl), Ala672 (alkyl), Ala410 (pi-alkyl)	Phe177	1.93	_
6m	−24	Ala410 (pi-sigma and pi-alkyl), Leu607 (pi-sigma, pi-alkyl and alkyl), Ala606 (alkyl),	Asn554, Gln557	1.63, 2.44	_

for finding effective LOX inhibitors. Docking conformations helped to recognize key interactions of the potent ligands of the series with the active sites of enzymes. This study has led to the discovery of core structure which would help in the development of potent drugs.

4. Experimental

4.1. Materials

Chemicals were purchased from Sigma-Aldrich and for thin layer chromatography (TLC), DC-Alufolien Silica Gel 60 F_{254} Merck was used. Melting points were determined over Gallen Kamp. Agilent Technologies Cary 630 FTIR spectrophotometer was used to run FTIR spectra. For ^{1}H (^{13}C) NMR spectra, Bruker Avance Instruments of 300 (75), 400 (100) or 500 (125) MHz were used. The analysis was carried out by dissolving compounds in $CDCl_3$/DMSO-d_6. The MS were recorded on JEOL JMS 600H or FTMS spectrometer. The CHN data was found out through Perkin Elmer 2400 Series II CHN/S Analyzer. Initial reactants **1** and **2** were synthesized following reported methods. Condensation reaction between 4-nitrophenylhydrazine hydrochloride and 2,4-petanedione in methanol afforded the initial precursor **1**. Further, nitro group was reduced to amine with the help of Sn/HCl to generate reactant **2**. Their physiochemical properties were also comparable with the literature reports [44].

4.2. Synthetic method

4.2.1. General procedure for the preparation of compound 6(a-m)

The reactant **2** (2.7 mmol) was first dissolved in acetic acid (15 mL) on heating. Afterwards, equivalent amounts (2.7 mmol) of substituted aldehyde **3**(**a-m**), benzil (**4**) and ammonium acetate (**5**) were added to the solution. The reaction mixture was refluxed for about 6 hrs and monitored through TLC. After reaction completion, the reaction contents were poured into cold water and neutralized with sodium carbonate solution to afford crude product **6**(**a-m**) which was further purified through column chromatography over silica gel by using *n*-hexane:ethyl acetate (in 8:2 ratio). These newly synthesized compounds **6**(**a-m**) were characterized by physical and spectral means.

4.2.2. 3,5-Dimethyl-1-(4-(2,4,5-triphenyl-1H-imidazol-1-yl)phenyl)-1H-pyrazole (6a)

White solid; m.p. 190–192 °C; Yield 73%; FTIR (ν_{max}-cm^{-1}; neat): 3055–2970 (C—H), 1602 (C═N), 1560 (C═C); ^{1}H NMR ($CDCl_3$, 500 MHz), δ: 2.26 (s, 3H; CH_3-5 Pyrazole), 2.27 (s, 3H; CH_3-3 Pyrazole), 5.99 (s, 1H; H-4 Pyrazole), 7.10 (d, 2H, J = 8.5 Hz; Ar-2H Pyrazole), 7.14–7.16 (m, 2H; Ar^2-2H), 7.19–7.22 (m, 1H; Ar^2-H), 7.24–7.29 (m, 8H; Ar^1-3H, Ar^2-2H & Ar^3-3H), 7.35 (d, 2H, J = 8.5 Hz; Ar-2H Imidazole), 7.46–7.48 (m, 2H; Ar^1-2H), 7.61 (d, 2H, J = 7.4 Hz; Ar^3-2H); ^{13}C NMR ($CDCl_3$, 75 MHz), δ: 12.76 (CH_3-5 Pyrazole), 13.59 (CH_3-3 Pyrazole), 107.88 (CH-4 Pyrazole), 124.75, 126.92, 127.57, 128.31, 128.36, 128.64, 128.70, 129.07, 129.21, 130.05, 130.38, 130.90, 131.25, 134.02, 135.56, 138.25, 139.57, 139.72, 147.01 (C-2 Imidazole), 149.72 (C-3 Pyrazole); MS (ESI): *m/z* (%) 467.2 ([M + H]$^+$, 100), 489.2 ([M + Na]$^+$, 25.1); Anal. Calcd. For $C_{32}H_{26}N_4$: C, 82.38; H, 5.62; N, 12.01%. Found: C, 82.29; H, 5.46; N, 11.93%.

4.2.3. 3,5-Dimethyl-1-(4-(2-(naphthalen-1-yl)-4,5-diphenyl-1H-imidazol-1-yl)phenyl)-1H-pyrazole (6b)

White solid; m.p. 183–185 °C; Yield 70%; FTIR (ν_{max}-cm^{-1}; neat): 3050–2955 (C—H), 1600 (C═N), 1555 (C═C); ^{1}H NMR ($CDCl_3$, 500 MHz), δ: 2.09 (s, 3H; CH_3-5 Pyrazole), 2.21 (s, 3H; CH_3-3 Pyrazole), 5.91 (s, 1H; H-4 Pyrazole), 6.94 (d, 2H, J = 8.2 Hz; Ar-2H Pyrazole), 7.11 (d, 2H, J = 8.2 Hz; Ar-2H Imidazole), 7.21–7.28 (m, 8H; Ar^1-3H, Ar^2-5H), 7.32–7.35 (m, 1H; H-7 Ar^3), 7.38–7.40 (m, 1H; H-6 Ar^3), 7.44–7.46 (m, 2H; H-1 & H-2 Ar^3), 7.67 (d, 2H, J = 7.4 Hz; Ar^1-H), 7.81–7.82 (m, 2H; H-4 & H-5 Ar^3), 8.13–8.14 (m, 1H; H-8 Ar^3); ^{13}C NMR ($CDCl_3$, 125 MHz), δ: 12.54 (CH_3-5 Pyrazole), 13.52 (CH_3-3 Pyrazole), 107.64 (CH-4 Pyrazole), 124.39, 124.82, 126.17, 126.19, 126.84, 126.90, 127.65, 127.98, 128.30, 128.32, 128.39, 128.74, 129.67, 129.72, 129.94, 130.57, 131.18, 132.75, 133.72, 134.28, 135.24, 138.21, 139.16, 139.49, 146.33 (C-2 Imidazole), 149.53 (C-3 Pyrazole); MS (ESI): *m/z* (%) 517.2 ([M + H]$^+$, 100), 539.2 ([M + Na]$^+$, 42.2); Anal. Calcd. For $C_{36}H_{28}N_4$: C, 83.69; H, 5.46; N, 10.84%. Found: C, 83.51; H, 5.38; N, 10.91%.

4.2.4. 1-(4-(2-(4-Fluorophenyl)-4,5-diphenyl-1H-imidazol-1-yl)phenyl)-3,5-dimethyl-1H-pyrazole (6c)

White solid; m.p. 178–180 °C; Yield: 71%; FTIR (ν_{max}-cm^{-1}; neat): 3056–2970 (C—H), 1599 (C═N), 1560 (C═C); ^{1}H NMR ($CDCl_3$, 500 MHz), δ: 2.27 (s, 3H; CH_3-5 Pyrazole), 2.27 (s, 3H; CH_3-3 Pyrazole), 6.00 (s, 1H; H-4 Pyrazole), 6.96 (t, 2H, J = 8.7 Hz ; Ar^3-2H), 7.09 (d, 2H, J = 8.6 Hz; Ar-2H Pyrazole), 7.14 (dd, 2H, J = 7.8, 2.0 Hz; Ar^2-2H), 7.18–7.21 (m, 1H; Ar^2-1H), 7.22–7.27 (m, 5H; Ar^1-3H & Ar^2-2H), 7.37 (d, 2H, J = 8.6 Hz; Ar-2H Imidazole), 7.45 (dd, 2H, J = 8.7, 5.4 Hz; Ar^3-2H), 7.59 (d, 2H, J = 7.2 Hz; Ar^1-2H); ^{13}C NMR ($CDCl_3$, 125 MHz), δ: 12.80 (CH_3-5 Pyrazole), 13.59 (CH_3-3 Pyrazole), 107.98 (CH-4 Pyrazole), 115.49 (d, 2C, J (^{13}C-^{19}F) = 22.7 Hz, CH-3 Ar^3 & CH-5 Ar^3), 124.80, 126.47, 126.96, 127.51, 128.34, 128.41, 128.67, 129.06, 130.35, 130.95, 131.08 (d, 2C, J (^{13}C-^{19}F) = 8.3 Hz, CH-2 Ar^3 & CH-6 Ar^3), 131.23, 134.06, 135.43, 138.36, 139.57, 139.85 146.14 (C-2 Imidazole), 149.82 (C-3 Pyrazole), 162.94 (d, 2C, J (^{13}C-^{19}F) = 249.2 Hz, C-F); MS (ESI): *m/z* (%) 485.2 ([M + H]$^+$, 100), 507.1 ([M + Na]$^+$, 58.0); Anal. Calcd. For $C_{32}H_{25}FN_4$: C, 79.32; H, 5.20; N, 11.56%. Found: C, 79.24; H, 5.09; N, 11.60%.

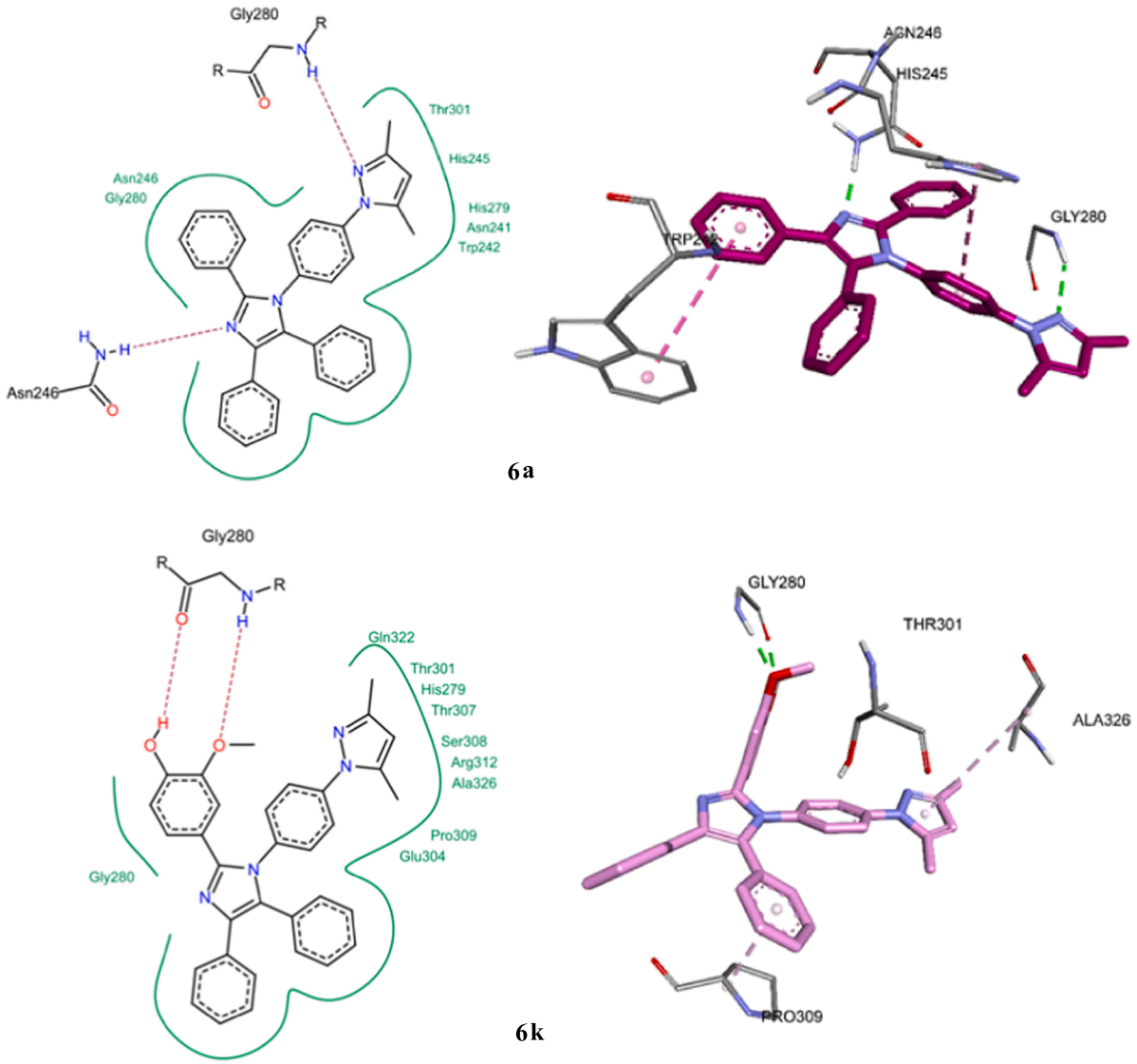

Fig. 5. Docked conformations of α-glucosidase inhibitors **6a** and **6k**.

4.2.5. 1-(4-(2-(4-Chlorophenyl)-4,5-diphenyl-1H-imidazol-1-yl)phenyl)-3,5-dimethyl-1H-pyrazole ***(6d)***

White solid; m.p. 185–187 °C; Yield 68%; FTIR (ν_{max}-cm^{-1}; neat): 3052–2950 (C—H), 1590 (C═N), 1555 (C═C); ^{1}H NMR ($CDCl_3$, 300 MHz), δ: 2.28 (s, 6H; 2 × CH_3 Pyrazole), 6.00 (s, 1H; H-4 Pyrazole), 7.10 (d, 2H, J = 8.8 Hz; Ar-2H Pyrazole), 7.12–7.15 (m, 2H; Ar^2-2H), 7.22–7.28 (m, 8H; Ar^1-3H, Ar^2-3H & Ar^3-2H), 7.37–7.42 (m, 4H; Ar-2H Imidazole & Ar^3-2H), 7.59 (dd, 2H, J = 8.2, 1.8 Hz; Ar^1-2H); ^{13}C NMR ($CDCl_3$, 75 MHz), δ: 12.84 (CH_3-5 Pyrazole), 13.60 (CH_3-3 Pyrazole), 108.04 (CH-4 Pyrazole), 124.82, 127.05, 127.53, 128.36, 128.49, 128.66, 128.69, 129.02, 130.18, 130.36, 131.22, 133.87, 134.85 (C-Cl), 135.29, 138.47, 139.58, 139.97, 145.85 (C-2 Imidazole), 149.85 (C-3 Pyrazole); MS (ESI): m/z (%) 501.1 ([M + H]$^+$, 100), 502.1 ([M + 2]$^+$, 31.2), 503.2 ([M + H + 2]$^+$, 29.1), 523.1 ([M + Na]$^+$, 6); Anal. Calcd. For $C_{32}H_{25}ClN_4$: C, 76.71; H, 5.03; N, 11.18%. Found: C, 76.59; H, 4.91; N, 11.26%.

4.2.6. 1-(4-(2-(4-Bromophenyl)-4,5-diphenyl-1H-imidazol-1-yl)phenyl)-3,5-dimethyl-1H-pyrazole ***(6e)***

White solid; m.p. 180–182 °C; Yield 71%; FTIR (ν_{max}-cm^{-1}; neat): 3050–2957 (C—H), 1603 (C═N), 1559 (C═C); ^{1}H NMR ($CDCl_3$, 500 MHz), δ: 2.26 (s, 6H; 2 × CH_3), 5.98 (s, 1H; H-4 Pyrazole), 7.08 (d, 2H, J = 8.6 Hz; Ar-2H Pyrazole), 7.12 (d, 2H, J = 6.4, 1.5 Hz; Ar^2-2H), 7.17–7.18 (m, 1H; Ar^1-1H), 7.22–7.25 (m, 5H; Ar-2H Imidazole & Ar^2-3H), 7.31 (d, 2H, J = 8.5 Hz; Ar^3-2H), 7.35–7.38 (m, 4H; Ar^1-2H & Ar^3-2H), 7.56 (d, 2H, J = 7.3 Hz; Ar^1-2H); ^{13}C NMR ($CDCl_3$, 125 MHz), δ: 12.68 (CH_3-5 Pyrazole), 13.45 (CH_3-3 Pyrazole), 107.86 (CH-4 Pyrazole), 122.81 (C-Br), 124.67, 126.78, 127.32, 128.19, 128.26, 128.52, 128.89, 129.29, 130.23, 130.36, 131.08, 131.14, 131.42, 134.10, 135.32, 138.67, 139.42, 139.78, 145.80 (C-2 Imidazole), 149.69 (C-3 Pyrazole); MS (EI): m/z (%) 544.0 (M$^+$, 100), 546.0 ([M + 2]$^+$, 100); Anal. Calcd. For $C_{32}H_{25}BrN_4$: C, 70.46; H, 4.62; N, 10.27%. Found: C, 70.31; H, 4.53; N, 10.16%.

4.2.7. 4-(1-(4-(3,5-Dimethyl-1H-pyrazol-1-yl)phenyl)-4,5-diphenyl-1H-imidazol-2-yl)phenol ***(6f)***

White solid; m.p. 234–236 °C; Yield 65%; FTIR (ν_{max}-cm^{-1}; neat): 3160 (br., OH), 3078–2924 (C—H), 1611 (C═N), 1556 (C═C), 1235 (C—O); ^{1}H NMR (DMSO-d_6, 400 MHz), δ: 2.14 (s, 3H; CH_3-5 Pyrazole), 2.23 (s, 3H; CH_3-3 Pyrazole), 6.05 (s, 1H; H-4 Pyrazole), 6.68 (d, 2H, J = 8.4 Hz; Ar^3-2H), 7.15–7.17 (m, 1H; Ar^2-1H), 7.21–7.23 (m, 6H; Ar-2H Pyrazole & Ar^2-4H), 7.30–7.31 (m, 5H; Ar^1-3H & Ar^3-2H), 7.42 (d, 2H, J = 8.4 Hz; Ar-2H Imidazole), 7.49 (d, 2H, J = 7.4 Hz; Ar^1-2H), 9.67 (br. s, 1H; OH); ^{13}C NMR (DMSO-d_6, 100 MHz), δ: 12.20 (CH_3-5 Pyrazole), 13.20 (CH_3-3 Pyrazole), 107.56 (CH-4 Pyrazole), 114.98, 121.10, 124.07, 126.31, 128.09, 128.31, 128.44, 129.44, 129.83,

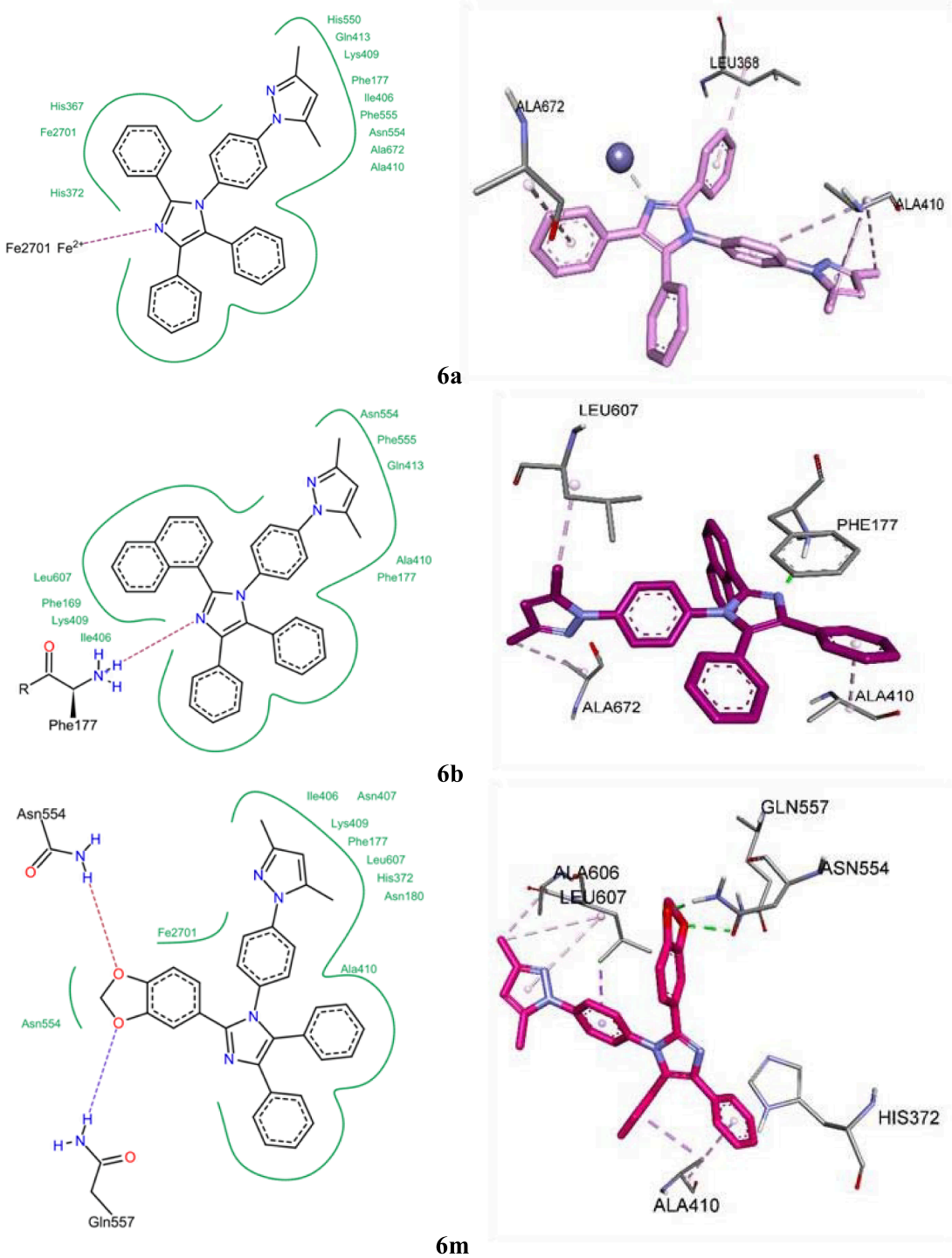

Fig. 6. Docked conformations of LOX inhibitors **6a**, **6b** and **6m**.

130.49, 130.53, 131.12, 134.49, 135.15, 136.48, 139.19, 139.30, 146.51 (C-2 Imidazole), 148.27 (C-3 Pyrazole), 157.66 (C-OH); MS (EI): *m/z* (%) 482.1 (M^+, 100); Anal. Calcd. For $C_{32}H_{26}N_4O$: C, 79.64; H, 5.43; N, 11.61%. Found: C, 79.45; H, 5.38; N, 11.62%.

*4.2.8. 1-(4-(2-(4-Methoxyphenyl)-4,5-diphenyl-1H-imidazol-1-yl) phenyl)-3,5-dimethyl-1H-pyrazole (**6g**)*

White solid; m.p. 201–203 °C; Yield 70%; FTIR (ν_{max}-cm^{-1}; neat): 3052–2948 (C—H), 1609 (C═N), 1563 (C═C), 1252 (Ar^3-O), 1025 (C—O); ^{1}H NMR (DMSO-d_6, 400 MHz), δ: 2.14 (s, 3H; CH_3-5 Pyrazole), 2.23 (s, 3H; CH_3-3 Pyrazole), 3.72 (s, 3H; —OCH_3), 6.06 (s, 1H; H-4 Pyrazole), 6.87 (d, 2H, $J = 8.7$ Hz; Ar^3-2H), 7.17–7.18 (m, 1H; Ar^2-1H), 7.22–7.25 (m, 4H; Ar-2H Pyrazole & Ar^2-2H), 7.30–7.36 (m, 7H; Ar^1-3H, Ar^2-2H & Ar^3-2H), 7.44 (d, 2H, $J = 8.5$ Hz; Ar-2H Imidazole), 7.49 (d, 2H, $J = 7.6$ Hz; Ar^1-2H); ^{13}C NMR (DMSO-d_6, 100 MHz), δ: 12.24 (CH_3-5 Pyrazole), 13.20 (CH_3-3 Pyrazole), 55.11 (—OCH_3), 107.62 (CH-4 Pyrazole), 113.67, 122.67, 124.04, 126.32, 126.38, 128.11, 128.37, 128.45, 129.45, 129.71, 130.40, 130.80, 131.12, 134.42, 135.03, 136.61, 139.28, 139.33, 146.07 (C-2 Imidazole), 148.30 (C-3 Pyrazole), 159.27 (C-OCH_3); MS (EI): *m/z* (%) 496.1 (M^+, 100); Anal. Calcd. For

$C_{33}H_{28}N_4O$: C, 79.81; H, 5.68; N, 11.28%. Found: C, 79.92; H, 5.61; N, 11.32%.

4.2.9. 4-(1-(4-(3,5-Dimethyl-1H-pyrazol-1-yl)phenyl)-4,5-diphenyl-1H-imidazol-2-yl)benzonitrile (6h)

White solid; m.p. 261–263 °C; Yield 77%; FTIR (ν_{max}-cm^{-1}; neat): 3060–2930 (C—H), 2229 (C≡N), 1602 (C=N), 1560 (C=C); ^{1}H NMR ($CDCl_3$, 500 MHz), δ: 2.26 (s, 3H; CH_3-5 Pyrazole), 2.27 (s, 3H; CH_3-3 Pyrazole), 5.99 (s, 1H; H-4 Pyrazole), 7.11 (d, 2H, J = 8.7 Hz; Ar-2H Pyrazole), 7.12–7.14 (m, 2H; Ar^2-2H), 7.20–7.27 (m, 6H; Ar^1-3H & Ar^2-3H), 7.40 (d, 2H, J = 8.7 Hz; Ar-2H Imidazole), 7.52 (d, 2H, J = 8.5 Hz; Ar^3-2H), 7.56 (dd, 2H, J = 7.0, 1.0 Hz; Ar^1-2H), 7.57 (d, 2H, J = 8.5 Hz; Ar^3-2H); ^{13}C NMR ($CDCl_3$, 125 MHz), δ: 12.71 (CH_3-5 Pyrazole), 13.42 (CH_3-3 Pyrazole), 108.03 (CH-4 Pyrazole), 111.66 (C-C≡N), 118.52 (C≡N), 124.76, 127.01, 127.24, 128.24, 128.50, 128.58, 128.80, 128.97, 129.82, 131.02, 131.96, 132.11, 133.76, 134.52, 134.95, 139.25, 139.41, 140.10 (C-2 Imidazole), 144.64, 149.82 (C-3 Pyrazole); MS (EI): m/z (%) 491.2 (M$^+$, 100); Anal. Calcd. For $C_{33}H_{25}N_5$: C, 80.63; H, 5.13; N, 14.25%. Found: C, 80.66; H, 5.06; N, 14.13%.

4.2.10. 3,5-Dimethyl-1-(4-(2-(4-nitrophenyl)-4,5-diphenyl-1H-imidazol-1-yl)phenyl)-1H-pyrazole (6i)

Yellow solid; m.p. 202–204 °C; Yield 78%; FTIR (ν_{max}-cm^{-1}; neat): 3059–2940 (C—H), 1601 (C=N), 1555 (C=C), 1517 & 1350 (NO_2); ^{1}H NMR ($CDCl_3$, 300 MHz), δ: 2.29 (s, 3H; CH_3-5 Pyrazole), 2.31 (s, 3H; CH_3-3 Pyrazole), 6.02 (s, 1H; H-4 Pyrazole), 7.15–7.17 (m, 4H; Ar-2H Pyrazole & Ar^2-2H), 7.24–7.28 (m, 6H; Ar^1-3H & Ar^2-3H), 7.45 (d, 2H, J = 8.7 Hz; Ar-2H Imidazole), 7.60 (d, 2H, J = 6.6 Hz; Ar^1-2H), 7.68 (d, 2H, J = 8.7 Hz; Ar^3-2H), 8.12 (d, 2H, J = 8.7 Hz; Ar^3-2H); ^{13}C NMR ($CDCl_3$, 125 MHz), δ: 12.78 (CH_3-5 Pyrazole), 13.43 (CH_3-3 Pyrazole), 108.15 (CH-4 Pyrazole), 123.50, 124.59, 124.76, 127.33, 127.38, 128.32, 128.68, 128.74, 128.80, 129.38, 130.99, 132.37, 132.93, 134.48, 135.52, 138.84, 139.44, 140.33 (C-2 Imidazole), 144.15 (Ar^3-C-NO_2), 147.32 (C-3 Pyrazole), 149.90 (Ar^3-C-Imidazole); MS (EI): m/z (%) 511.0 (M$^+$, 100); Anal. Calcd. For $C_{32}H_{25}N_5O_2$: C, 75.13; H, 4.93; N, 13.69%. Found: C, 75.02; H, 4.74; N, 13.71%.

4.2.11. 4-(1-(4-(3,5-Dimethyl-1H-pyrazol-1-yl)phenyl)-4,5-diphenyl-1H-imidazol-2-yl)-N,N-dimethylaniline (6j)

White solid; m.p. 174–176 °C; Yield 66%; FTIR (ν_{max}-cm^{-1}; neat): 3053–2930 (C—H), 1606 (C=N), 1570 (C=C), 1359 (C—N); ^{1}H NMR (DMSO-d_6, 400 MHz), δ: 2.14 (s, 3H; CH_3-5 Pyrazole), 2.24 (s, 3H; CH_3-3 Pyrazole), 2.88 (s, 6H; -N(CH_3)$_2$), 6.06 (s, 1H; H-4 Pyrazole), 6.60 (d, 2H, J = 8.6 Hz; Ar^3-2H), 7.15–7.17 (m, 1H; Ar^2-1H), 7.23–7.25 (m, 6H; Ar-2H Pyrazole & Ar^2-4H), 7.29–7.32 (m, 5H; Ar^1-3H & Ar^3-2H), 7.44 (d, 2H, J = 8.3 Hz; Ar-2H Imidazole), 7.49 (d, 2H, J = 7.5 Hz; Ar^1-2H); ^{13}C NMR (DMSO-d_6, 100 MHz), δ: 12.27 (CH_3-5 Pyrazole), 13.21 (CH_3-3 Pyrazole), 39.71 (-N(CH_3)$_2$), 107.60 (CH-4 Pyrazole), 111.38, 117.52, 124.00, 126.25, 126.30, 128.07, 128.24, 128.41, 129.08, 129.49, 130.36, 130.59, 131.15, 134.59, 135.37, 136.40, 139.16, 139.31, 146.79 (C-2 Imidazole), 148.27 (C-3 Pyrazole), 149.98 (C—N(CH_3)$_2$); MS (EI): m/z (%) 509.1 (M$^+$, 100); Anal. Calcd. For $C_{34}H_{31}N_5$: C, 80.13; H, 6.13; N, 13.74%. Found: C, 79.95; H, 6.08; N, 13.73%.

4.2.12. 4-(1-(4-(3,5-Dimethyl-1H-pyrazol-1-yl)phenyl)-4,5-diphenyl-1H-imidazol-2-yl)-2-methoxyphenol (6k)

White solid; m.p. 228–230 °C; Yield 60%; FTIR (ν_{max}-cm^{-1}; neat): 3057 (br., OH), 3040–2933 (C—H), 1605 (C=N), 1596 (C=C), 1269 & 1033 (Ar^3-O-CH_3); ^{1}H NMR ($CDCl_3$, 500 MHz), δ: 2.24 (s, 3H; CH_3-5 Pyrazole), 2.25 (s, 3H; CH_3-3Pyrazole), 3.77 (s, 3H; —OCH_3), 5.74 (br. s, 1H; OH), 5.97 (s, 1H; H-4 Pyrazole), 6.70 (d, 1H, J_{ab} = 8.3 Hz; Ar^3-1H), 6.74 (dd, 1H, J_{ab} = 8.3 & J_{bc} = 1.8 Hz; Ar^3-1H), 7.09 (d, 2H, J = 8.7 Hz; Ar-2H Pyrazole), 7.12 (dd, 1H, J = 7.6, 1.5 Hz; Ar^2-1H), 7.15 (d, 1H, J = 1.8 Hz; Ar^3-1H), 7.17–7.18 (m, 1H; Ar^2-1H), 7.21–7.24 (m, 5H; Ar^1-3H & Ar^2-2H), 7.34 (d, 2H, J = 8.7 Hz; Ar-2H Imidazole), 7.57 (dd, 2H, J = 7.2, 1.4 Hz; Ar-2H); ^{13}C NMR ($CDCl_3$, 125 MHz), δ: 12.58 (CH_3-5 Pyrazole), 13.40 (CH_3-3 Pyrazole), 55.81 (—OCH_3), 107.73 (CH-4 Pyrazole), 111.95, 114.11, 122.15, 122.37, 124.57, 126.61, 127.40, 128.07, 128.12, 128.44, 128.71, 129.00, 130.37, 130.43, 131.10, 134.20, 135.78, 138.05, 139.38, 146.27 (C-2 Imidazole), 146.44 (C-OCH_3), 147.10 (C-3 Pyrazole), 149.57 (C-OH); MS (ESI): m/z (%) 512.3 (M + H$^+$, 100); Anal. Calcd. For $C_{33}H_{28}N_4O_2$: C, 77.32; H, 5.51; N, 10.93%. Found: C, 77.27; H, 5.44; N, 11.01%.

4.2.13. 5-Bromo-2-(1-(4-(3,5-dimethyl-1H-pyrazol-1-yl)phenyl)-4,5-diphenyl-1H-imidazol-2-yl)phenol (6l)

White solid; m.p. 192–194 °C; Yield 58%; FTIR (ν_{max}-cm^{-}1; neat): 3064 (br., OH), 3050–2921 (C—H), 1604 (C=N), 1578 (C=C); ^{1}H NMR ($CDCl_3$, 500 MHz), δ: 2.28 (s, 3H; CH_3-5 Pyrazole), 2.35 (s, 3H; CH_3-3 Pyrazole), 6.01 (s, 1H; H-4 Pyrazole), 6.56 (d, 1H, J = 2.4 Hz; Ar^3-1H), 6.94 (d, 1H, J = 8.8 Hz; Ar^3-1H), 7.16 (dd, 2H, J = 7.9, 1.5 Hz; Ar^2-2H), 7.20 (t, 1H, J = 4.0, 2.5 Hz; Ar^1-1H), 7.22 (t, 1H, J = 2.5, 1.5 Hz; Ar^2-1H), 7.23–7.28 (m, 7H; Ar-2H Pyrazole, Ar^1-2H, Ar^2-2H & Ar^3-1H), 7.49 (d, 2H, J = 8.7 Hz; Ar-2H Imidazole), 7.49–7.51 (m, 2H; Ar^1-2H), 13.41 (br. s, 1H; OH); ^{13}C NMR ($CDCl_3$, 125 MHz), δ: 12.68 (CH_3-5 Pyrazole), 13.45 (CH_3-3 Pyrazole), 107.89 (CH-4 Pyrazole), 109.55, 114.36, 119.52, 125.60, 126.88, 127.25, 128.33, 128.45, 128.79, 128.90, 129.13, 129.16, 130.78, 131.22, 132.49, 132.66, 135.08, 135.59, 139.85, 140.68, 143.63 (C-2 Imidazole), 149.84 (C-3 Pyrazole), 157.52 (C-OH); MS (ESI): m/z (%) 561.2 ([M + H]$^+$, 98.1), 563.2 ([M + H + 2]$^+$, 100); Anal. Calcd. For $C_{32}H_{25}BrN_4O$: C, 68.45; H, 4.49; N, 9.98%. Found: C, 68.38; H, 4.45; N, 9.83%.

4.2.14. 1-(4-(2-(Benzo[d][1,3]dioxol-5-yl)-4,5-diphenyl-1H-imidazol-1-yl)phenyl)-3,5-dimethyl-1H-pyrazole (6m)

White solid; m.p. 182–184 °C; Yield 70%; FTIR (ν_{max}-cm^{-1}; neat): 3056–2984 (C—H), 1601 (C=N), 1558 (C=C), 1034 (C—O); ^{1}H NMR (DMSO-d_6, 400 MHz), δ: 2.14 (s, 3H; CH_3-5 Pyrazole), 2.22 (s, 3H; CH_3-3 Pyrazole), 6.01 (s, 2H; CH_2), 6.06 (s, 1H; H-4 Pyrazole), 6.85 (d, 1H, J = 8.0 Hz; Ar^3-1H), 6.89 (d, 1H, J = 8.0 Hz; Ar^3-1H), 6.93 (s, 1H; Ar^3-1H), 7.17–7.18 (m, 1H; Ar^2-1H), 7.22–7.26 (m, 4H; Ar-2H Pyrazole & Ar^2-2H), 7.30–7.35 (m, 5H; Ar^1-3H & Ar^2-2H), 7.44 (d, 2H, J = 8.4 Hz; Ar-2H Imidazole), 7.49 (d, 2H, J = 7.5 Hz; Ar^1-2H); ^{13}C NMR (DMSO-d_6, 100 MHz), δ: 12.20 (CH_3-5 Pyrazole), 13.19 (CH_3-3 Pyrazole), 101.29 (—CH_2), 107.60 (CH-4 Pyrazole), 108.09, 108.50, 122.63, 124.11, 126.33, 126.42, 128.11, 128.41, 128.46, 129.46, 130.31, 130.94, 131.11, 134.32, 134.94, 136.58, 139.32, 145.86 (C-2 Imidazole), 147.05 (C-3 Pyrazole), 147.41, 148.31; MS (EI): m/z (%) 510.2 (M$^+$, 100); Anal. Calcd. For $C_{33}H_{26}N_4O_2$: C, 77.63; H, 5.13; N, 10.97%. Found: C, 77.71; H, 5.11; N, 11.16%.

4.3. Enzyme inhibition assays

To determine the inhibition of selected enzymes, we used our previously reported protocols [37,38]. Study of α-glucosidase inhibition was carried out with respective enzyme isolated from *Saccharomyces cerevisiae* (Cat No. 5003-1KU Type I, Sigma USA) while the positive control was acarbose. For LOX inhibition, lipoxygenase enzyme isolated from *Glycine* max (Sigma, USA) was used and baicalein was the positive control. Compounds were dissolved in HPLC grade methanol and assays were carried out with different sample dilutions and run in triplicates. After calculating the inhibitory percentages, IC_{50} values were determined with the help of EZ-Fit Enzyme Kinetics Software from Perrella Scientific Inc.

4.4. Molecular docking

The crystal structure data of α-glucosidase from *Saccharomyces cerevisiae* is not yet available in protein data bank (PDB). Previously, we built its homology model, validated and reported [38–40,42]. Herein, this model was utilized for the docking studies. Whereas for LOX studies, the crystal structure was downloaded from the PDB (PDB ID: 3V99) and

docking was performed on BioSolveIT's LeadIT software [51]. The detailed studies regarding binding interactions were carried out with the most favorable conformations possessing the lowest binding energies. Discovery Studio Visualizer 3.5 was used for visualization of docked structures.

Declaration of Competing Interest

The authors declare that they have no known competing financial interests or personal relationships that could have appeared to influence the work reported in this paper.

Acknowledgements

F.C. is highly grateful to the Higher Education Commission of Pakistan (HEC) for their financial support during her research projects. A part of this research study was carried out from NRPU-4950 funded project to M.A. wherein W.S. worked as research assistant.

Appendix A. Supplementary material

Supplementary data to this article can be found online at https://doi.org/10.1016/j.bioorg.2021.104686.

References

[1] a) L.D. Luca, Naturally occurring and synthetic imidazoles: their chemistry and their biological activities, Curr. Med. Chem. 13 (2006) 1–23;
b) V. Kumar, K. Kaur, G.K. Gupta, A.K. Sharma, Pyrazole containing natural products: synthetic preview and biological significance, Eur. J. Med. Chem. 69 (2013) 735–753.

[2] a) Y. Xue, R. Wang, C. Zheng, G. Liu, S. Pu, A new multi-addressable molecular switch based on a photochromic diarylethene with a thieno-imidazole unit, Tetrahedron Lett. 57 (2016) 1877–1881;
b) N.A.A. Elkanzi, J. Chin. Chem. Soc. 65 (2018) 189–204;
c) K. Rustler, P. Nitschke, S. Zahnbrecher, J. Zach, S. Crespi, B. König, Photochromic evaluation of 3(5)-arylazo-1H-pyrazoles, J. Organic Chem. 85 (2020) 4079–4088.

[3] a) M.S. Ahmad, M. Khalid, M.A. Shaheen, M.N. Tahir, M.U. Khan, A.C.C. Braga, H. A. Shad, Synthesis and XRD, FT-IR vibrational, UV-Vis, and nonlinear optical exploration of novel tetra-substituted imidazole derivatives: a synergistic experimental-computational analysis, J. Phys. Chem. Solids 115 (2018) 265–276;
b) C.W. Ghanavatkar, V.R. Mishra, N. Sekar, E. Mathew, S.S. Thomas, I.H. Joe, Benzothiazole pyrazole containing emissive azo dyes decorated with ESIPT core: Linear and non linear optical properties, Z scan, optical limiting, laser damage threshold with comparative DFT studies, J. Mol. Struct. 1203 (2020), 127401;
c) G.H. Bae, S. Kim, N.K. Lee, A. Dagar, J.H. Lee, J. Lee, I. Kim, Facile approach to benzo [d] imidazole-pyrrolo [1, 2-a] pyrazine hybrid structures through double cyclodehydration and aromatization and their unique optical properties with blue emission, RSC Adv. 10 (2020) 7265–7288.

[4] a) D. Huang, A. Liu, W. Liu, X. Liu, Y. Ren, X. Zheng, H. Pei, J. Xiang, M. Huang, X. Wang, Synthesis and insecticidal activities of novel 1H-pyrazole-5-carboxylic acid derivatives, Heterocycl. Commun. 23 (2017) 455–460;
b) L. Chen, B. Zhao, Z. Fan, X. Liu, Q. Wu, H. Li, H. Wang, Synthesis of novel 3,4-chloroisothiazole-based imidazoles as fungicides and evaluation of their mode of action, J. Agric. Food. Chem. 66 (2018) 7319–7327.

[5] X. Han, X. Ling, Y. Wang, T. Ma, C. Zhong, W. Hu, Y. Deng, Generation of nanoparticle, atomic-cluster, and single-atom cobalt catalysts from zeolitic imidazole frameworks by spatial isolation and their use in zinc–air batteries, Angew. Chem. 131 (2019) 5413–5418.

[6] M.M. Heravi, V. Zadsirjan, Prescribed drugs containing nitrogen heterocycles: an overview, RSC Adv. 10 (2020) 44247–44311.

[7] S. Sharma, D. Kumar, G. Singh, V. Monga, B. Kumar, Recent advancements in the development of heterocyclic anti-inflammatory agents, Eur. J. Med. Chem. 200 (2020), 112438.

[8] a) I. Ali, M.N. Lone, H.Y. Aboul-Enein, Imidazoles as potential anticancer agents, Med. Chem. Commun. 8 (2017) 1742–1773;
b) F.E. Bennani, L. Doudach, Y. Cherrah, Y. Ramli, K. Karrouchi, M.E.A. Faouzi, Overview of recent developments of pyrazole derivatives as an anticancer agent in different cell line, Bioorg. Chem. 97 (2020), 103470.

[9] a)V. Padmavathi, B.C. Venkatesh, A. Padmaja, A. Synthesis and antimicrobial activity of amido linked pyrrolyl and pyrazolyl-oxazoles, thiazoles and imidazoles, Eur. J. Med. Chem. 46 (2011) 5317–5326. b) D.V. Sowmya, S.S. Basha, P.U. M. Devi, Y. Lavanyalatha, A. Padmaja, V. Padmavathi, Synthesis, antimicrobial, and anti-inflammatory activities of acetamido pyrrolyl azoles, Med. Chem. Res. 26 (2017) 1010–1021.

[10] V. Pogaku, K. Gangarapu, S. Basavoju, K.K. Tatapudi, S.B. Katragadda, Design, synthesis, molecular modelling, ADME prediction and anti-hyperglycemic evaluation of new pyrazole-triazolopyrimidine hybrids as potent α-glucosidase inhibitors, Bioorg. Chem. 93 (2019), 103307.

[11] N. Arshad, M. Rafiq, R. Ujan, A. Saeed, S.I. Farooqi, F. Perveen, P.A. Channar, S. Ashraf, Q. Abbas, A. Ahmed, T. Hokelek, Synthesis, X-ray crystal structure elucidation and Hirschfeld surface analysis of *N*-((4-(1*H*-benzo [d] imidazole-2-yl) phenyl) carbamothioyl) benzamide: investigations for elastase inhibition, antioxidant and DNA binding potentials for biological applications, RSC Adv. 10 (2020) 20837–20851.

[12] a) R.A. Copeland, M.R. Harpel, P.J. Tummino, Targeting enzyme inhibitors in drug discovery, Expert Opin. Therapeutic Targets 11 (2007) 967–978;
b) X. Liang, Q. Wu, S. Luan, Z. Yin, C. He, L. Yin, Y. Zou, Z. Yuan, L. Li, X. Song, M. He, A comprehensive review of topoisomerase inhibitors as anticancer agents in the past decade, Eur. J. Med. Chem. 171 (2019) 129–168;
c) S. Kandasamy, P. Subramani, S. Subramani, J.M. Jayaraj, G. Prasanth, K. Srinivasan, K. Muthusamy, V. Rajakannan, R. Vilwanathan, Design and synthesis of imidazole based zinc binding groups as novel small molecule inhibitors targeting histone deacetylase enzymes in lung cancer, J. Mol. Struct. 1214 (2020), 128177;
d) M. Adib, F. Peytam, R. Shourgeshty, M.M. Khanaposhtani, M. Jahani, S. Imanparast, M.A. Faramarzi, B. Larijani, A.A. Moghadamnia, E.N. Esfahani, F. Bandarian, Design and synthesis of new fused carbazole-imidazole derivatives as anti-diabetic agents: in vitro α-glucosidase inhibition, kinetic, and in silico studies, Bioorg. Med. Chem. Lett. 29 (2019) 713–718.

[13] P.A. Channar, A. Saeed, F.A. Larik, B. Batool, S. Kalsoom, M.M. Hasan, M.F. Erben, H.R. El-Seedi, M. Ali, Z. Ashraf, Synthesis of aryl pyrazole *via* Suzuki coupling reaction, *in vitro* mushroom tyrosinase enzyme inhibition assay and *in silico* comparative molecular docking analysis with Kojic acid, Bioorg. Chem. 79 (2018) 293–300.

[14] R. Rafique, K.M. Khan, S. Chigurupati, A. Wadood, A.U. Rehman, A. Karunanidhi, S. Hameed, M. Taha, M. Al-Rashida, Synthesis of new indazole based dual inhibitors of α-glucosidase and α-amylase enzymes, their *in vitro*, *in silico* and kinetics studies, Bioorg. Chem. 94 (2020), 103195.

[15] F. Turkan, A. Çetin, P. Taslimi, M. Karaman, I. Gulçin, Synthesis, biological evaluation and molecular docking of novel pyrazole derivatives as potent carbonic anhydrase and acetylcholinesterase inhibitors, Bioorg. Chem. 86 (2019) 420–427.

[16] H. Liu, Z.W. Chu, D.G. Xia, H.Q. Cao, X.H. Lv, Discovery of novel multi-substituted benzo-indole pyrazole schiff base derivatives with antibacterial activity targeting DNA gyrase, Bioorg. Chem. 99 (2020), 103807.

[17] S. Ullah, M.I. El-Gamal, S. Zaib, H.S. Anbar, S.O. Zaraei, R.M. Sbenati, J. Pelletier, J. Sévigny, C.H. Oh, J. Iqbal, Synthesis, biological evaluation, and docking studies of new pyrazole-based thiourea and sulfonamide derivatives as inhibitors of nucleotide pyrophosphatase/phosphodiesterase, Bioorg. Chem. 99 (2020), 103783.

[18] a) G.S. Hassan, D.E.A. Rahman, E.A. Abdelmajeed, R.H. Refaey, M.A. Salem, Y. M. Nissan, New pyrazole derivatives: Synthesis, anti-inflammatory activity, cyclooxygenase inhibition assay and evaluation of mPGES, Eur. J. Med. Chem. 171 (2019) 332–342;
b) M.R. Kumar, V.V. Dhayabaran, N. Sudhapriya, A. Manikandan, D.A. Gideon, S. Annapoorani, p-TSA.H2O mediated one-pot, multi-component synthesis of isatin derived imidazoles as dual-purpose drugs against inflammation and cancer, Bioorg. Chem. 102 (2020), 104046.

[19] a) B. Usman, N. Sharma, S. Satija, M. Mehta, M. Vyas, G.L. Khatik, N. Khurana, P. M. Hansbro, K. Williams, K. Dua, Recent developments in alpha-glucosidase inhibitors for management of type-2 diabetes: An update, Curr. Pharm. Des. 25 (2019) 2510–2525;
b) J. Dowarah, V.P. Singh, Anti-diabetic drugs recent approaches and advancements, Bioorg. Med. Chem. 28 (2020), 115263.

[20] M. Dhameja, P. Gupta, Synthetic heterocyclic candidates as promising α-glucosidase inhibitors: An overview, Eur. J. Med. Chem. 176 (2019) 343–377.

[21] F. Rahim, K. Zaman, M. Taha, H. Ullah, M. Ghufran, A. Wadood, W. Rehman, N. Uddin, S.A.A. Shah, M. Sajid, F. Nawaz, Synthesis, *in vitro* alpha-glucosidase inhibitory potential of benzimidazole bearing bis-Schiff bases and their molecular docking study, Bioorg. Chem. 94 (2020), 103394.

[22] a) M. Roza, A. Francke, Soyabean lipoxygenase: an iron-containing enzyme, Biochim. Biophys. Acta (BBA)-Enzymol. 327 (1973) 24–31;
b) R. Mashima, T. Okuyama, The role of lipoxygenases in pathophysiology; new insights and future perspectives, Redox Biol. 6 (2015) 297–310.

[23] a) J.Z. Haeggström, C.D. Funk, Lipoxygenase and leukotriene pathways: biochemistry, biology, and roles in disease, Chem. Rev. 111 (2011) 5866–5898;
b) A.Y. Chen, R.N. Adamek, B.L. Dick, C.V. Credille, C.N. Morrison, S.M. Cohen, Targeting metalloenzymes for therapeutic intervention, Chem. Rev. 119 (2019) 1323–1455.

[24] A. Orafaie, M. Mousavian, H. Orafai, H. Sadeghian, An overview of lipoxygenase inhibitors with approach of *in vivo* studies, Prostaglandins Other Lipid Mediat. 148 (2020), 106411.

[25] C. Hu, S. Ma, Recent development of lipoxygenase inhibitors as anti-inflammatory agents, MedChemComm 9 (2018) 212–225.

[26] S. Muthuraman, S. Sinha, C.S. Vasavi, K.M. Waidha, B. Basu, P. Munussami, M. M. Balamurali, M. Doble, R.S. Kumar, Design, synthesis and identification of novel coumaperine derivatives for inhibition of human 5-LOX: Antioxidant, pseudoperoxidase and docking studies, Bioorg. Med. Chem. 27 (2019) 604–619.

[27] I. Kostopoulou, A. Diassakou, E. Kavetsou, E. Kritsi, P. Zoumpoulakis, E. Pontiki, D. H. Litina, A. Detsi, Novel quinolinone-pyrazoline hybrids: synthesis and evaluation of antioxidant and lipoxygenase inhibitory activity, Mol. Diversity (2020) 1–18.

[28] Y.M. Omar, S.G. Abdel-Moty, H.H. Abdu-Allah, Further insight into the dual COX-2 and 15-LOX anti-inflammatory activity of 1,3,4-thiadiazole-thiazolidinone hybrids:

The contribution of the substituents at 5th positions is size dependent, Bioorg. Chem. 97 (2020), 103657.

[29] a) H. Sadeghian, A. Jabbari, 15-Lipoxygenase inhibitors: a patent review, Expert Opin. Ther. Pat. 26 (2016) 65–88;
b)Z. Hanáková, J. Hošek, Z. Kutil, V. Temml, P. Landa, T. Vaněk, D. Schuster, S. Dall'Acqua, J. Cvačka, O. Polanský, K. Šmejkal, Anti-inflammatory activity of natural geranylated flavonoids: Cyclooxygenase and lipoxygenase inhibitory properties and proteomic analysis, J. Nat. Products 80 (2017) 999–1006. c) N. Riaz, H.M. Rafiq, M. Saleem, B. Jabeen, M. Ashraf, I. Ahmed, T. Tahir, R. B. Tareen, Lipoxygenase and α-glucosidase inhibitory constituents of Phlomis stewartii, Chem. Nat. Compd. 55 (2019) 493–498;
d) H. Guo, I.C. Verhoek, G.G. Prins, R. van der Vlag, P.E. van der Wouden, R. van Merkerk, W.J. Quax, P. Olinga, A.K. Hirsch, F.J. Dekker, Novel 15-lipoxygenase-1 inhibitor protects macrophages from lipopolysaccharide-induced cytotoxicity, J. Med. Chem. 62 (2019) 4624–4637;
e) A.M. Ramírez, C.T. Farías, C.M. Collado, A.U. Moll, Study of two isoforms of lipoxygenase by kinetic assays, docking and molecular dynamics of a specialised metabolite isolated from the aerial portion of Lithrea caustica (Anacardiaceae) and its synthetic analogs, Phytochemistry 174 (2020), 112359.

[30] A. Barmak, K. Niknam, G. Mohebbi, Synthesis, structural studies, and α-glucosidase inhibitory, antidiabetic, and antioxidant activities of 2,3-dihydroquinazolin-4(1*H*)-ones derived from pyrazol-4-carbaldehyde and anilines, ACS Omega 4 (2019) 18087–18099.

[31] P. Singh, S. Mothilal, N. Kerru, A.S. Pillay, L. Gummidi, O.L. Erukainure, M. S. Islam, Comparative α-glucosidase and α-amylase inhibition studies of rhodanine-pyrazole conjugates and their simple rhodanine analogues, Med. Chem. Res. 28 (2019) 143–159.

[32] S.A. Ali, S.M. Awad, A.M. Said, S. Mahgoub, H. Taha, N.M. Ahmed, Design, synthesis, molecular modelling and biological evaluation of novel 3-(2-naphthyl)-1-phenyl-1*H*-pyrazole derivatives as potent antioxidants and 15-lipoxygenase inhibitors, J. Enzyme Inhib. Med. Chem. 35 (2020) 847–863.

[33] M.A. Shabaan, A.M. Kamal, S.I. Faggal, A.E. Elsahar, K.O. Mohamed, Synthesis and biological evaluation of pyrazolone analogues as potential anti-inflammatory agents targeting cyclooxygenases and 5-lipoxygenase, Arch. Pharm. 353 (2020) 1900308.

[34] M.T.E. Maghraby, O.M.A. Ghadir, S.G.A. Moty, A.Y. Ali, O.I. Salem, Novel class of benzimidazole-thiazole hybrids: The privileged scaffolds of potent anti-inflammatory activity with dual inhibition of cyclooxygenase and 15-lipoxygenase enzymes, Bioorg. Med. Chem. 28 (2020), 115403.

[35] A.S. Cornec, L. Monti, J. Kovalevich, V. Makani, M.J. James, K.G. Vijayendran, K. Oukoloff, Y. Yao, V.M.Y. Lee, J.Q. Trojanowski, A.B. Smith III, Multitargeted imidazoles: potential therapeutic leads for Alzheimer's and other neurodegenerative diseases, J. Med. Chem. 60 (2017) 5120–5145.

[36] O.S. Afifi, O.G. Shaaban, H.A.A. El Razik, S.E.A.S. Al-Dine, F.A. Ashour, A.A. El-Tombary, M.M. Abu-Serie, Synthesis and biological evaluation of purine-pyrazole hybrids incorporating thiazole, thiazolidinone or rhodanine moiety as 15-LOX inhibitors endowed with anticancer and antioxidant potential, Bioorg. Chem. 87 (2019) 821–837.

[37] S. Naureen, F. Chaudhry, N. Asif, M.A. Munawar, M. Ashraf, F.H. Nasim, H. Arshad, M.A. Khan, Discovery of indole-based tetraarylimidazoles as potent inhibitors of urease with low antilipoxygenase activity, Eur. J. Med. Chem. 102 (2015) 464–470.

[38] F. Chaudhry, S. Naureen, R. Huma, A. Shaukat, M. al-Rashida, N. Asif, M. Ashraf, M.A. Munawar, M.A. Khan, In search of new α-glucosidase inhibitors: Imidazolylpyrazole derivatives, Bioorganic Chem. 71 (2017) 102–109.

[39] a)F. Chaudhry, A.Q. Ather, M.J. Akhtar, A. Shaukat, M. Ashraf, M. al-Rashida, M.A. Munawar, M.A. Khan, Green synthesis, inhibition studies of yeast α-glucosidase and molecular docking of pyrazolylpyridazine amines, Bioorganic Chem., 71 (2017) 170–180. b) F. Chaudhry, S. Choudhry, R. Huma, M. Ashraf, M. Al-Rashida, R. Munir, R. Sohail, B. Jahan, M.A. Munawar, M.A. Khan, Hetarylcoumarins: Synthesis and biological evaluation as potent α-glucosidase inhibitors, Bioorg. Chem. 73 (2017) 1–9.

[40] F. Chaudhry, S. Naureen, M. Ashraf, M. Al-Rashida, B. Jahan, M.A. Munawar, M. A. Khan, Imidazole-pyrazole hybrids: Synthesis, characterization and *in-vitro* bioevaluation against α-glucosidase enzyme with molecular docking studies, Bioorg. Chem. 82 (2019) 267–273.

[41] N. Javid, R. Munir, F. Chaudhry, A. Imran, S. Zaib, A. Muzaffar, J. Iqbal, Exploiting oxadiazole-sulfonamide hybrids as new structural leads to combat diabetic complications via aldose reductase inhibition, Bioorg. Chem. 99 (2020), 103852.

[42] F. Chaudhry, S. Naureen, S. Choudhry, R. Huma, M. Ashraf, M. Al-Rashida, B. Jahan, M.H. Khan, F. Iqbal, M.A. Munawar, M.A. Khan, Evaluation of α-glucosidase inhibiting potentials with docking calculations of synthesized arylidene-pyrazolones, Bioorg. Chem. 77 (2018) 507–514.

[43] a) Z. Jaafar, S. Chniti, A.B. Sassi, H. Dziri, S. Marque, M. Lecouvey, R. Gharbi, M. Msaddek, Design and microwave-assisted synthesis of dimers of 1,5-benzodiazepine-1,2,3-triazole hybrids bearing alkyl/aryl spacers and their biological assessment, J. Mol. Struct. 1195 (2019) 689–701;
b) Z. Jin, L. Wang, H. Gao, Y.H. Zhou, Y.H. Liu, Y.Z. Tang, Design, synthesis and biological evaluation of novel pleuromutilin derivatives possessing acetamine phenyl linker, Eur. J. Med. Chem. 181 (2019), 111594;
c) H. Gao, X. Zhang, X.J. Pu, X. Zheng, B. Liu, G.X. Rao, C.P. Wan, Z.W. Mao, 2-Benzoylbenzofuran derivatives possessing piperazine linker as anticancer agents, Bioorg. Med. Chem. Lett. 29 (2019) 806–810.

[44] a) E.R. Tiekink, S.M. Wardell, J.L. Wardell, 3,5-Dimethyl-1-(4-nitrophenyl)-1H-pyrazole, Acta Crystallogr. Sect. E: Struct. Rep. Online 68 (2012);
b) K. Nagarajan, S.J. Shenoy, P.K. Talwalker, Synthesis and oral hypoglycemic properties of 3-(1-oxo-3-hydroxy-2-cyclohexen-2-yl)-4-oxo-4,5,6,7-tetrahydroindoles, Indian J. Chem. Section B-Organic Chem. Including Med. Chem. 28 (1989) 326–332.

[45] F. Compernolle, M. Dekeirel, M., Nitrogen elimination in the mass spectra of diphenyl and triphenyl-v-triazoles. Organic Mass Spectrometry, 5 (1971) 427-436.

[46] P.A. Channar, S. Afzal, S.A. Ejaz, A. Saeed, F.A. Larik, P.A. Mahesar, J. Lecka, J. Sévigny, M.F. Erben, J. Iqbal, Exploration of carboxy pyrazole derivatives: Synthesis, alkaline phosphatase, nucleotide pyrophosphatase/phosphodiesterase and nucleoside triphosphate diphosphohydrolase inhibition studies with potential anticancer profile, Eur. J. Med. Chem. 156 (2018) 461–478.

[47] F. Azimi, J.B. Ghasemi, H. Azizian, M. Najafi, M.A. Faramarzi, L. Saghaei, H. Sadeghi-aliabadi, B. Larijani, F. Hassanzadeh, M. Mahdavi, Design and synthesis of novel pyrazole-phenyl semicarbazone derivatives as potential α-glucosidase inhibitor: Kinetics and molecular dynamics simulation study, Int. J. Biol. Macromol. 166 (2021) 1082–1095.

[48] M.A. Abdelgawad, M.B. Labib, M. Abdel-Latif, Pyrazole-hydrazone derivatives as anti-inflammatory agents: Design, synthesis, biological evaluation, COX-1,2/5-LOX inhibition and docking study, Bioorg. Chem. 74 (2017) 212–220.

[49] D. Shahzad, A. Saeed, F.A. Larik, P.A. Channar, Q. Abbas, M.F. Alajmi, M.I. Arshad, M.F. Erben, M. Hassan, H. Raza, S.Y. Seo, Novel C-2 symmetric molecules as α-glucosidase and α-amylase inhibitors: Design, synthesis, kinetic evaluation, molecular docking and pharmacokinetics, Molecules 24 (2019) 1511.

[50] E.M. Gedawy, A.E. Kassab, A.M. El Kerdawy, Design, synthesis and biological evaluation of novel pyrazole sulfonamide derivatives as dual COX-2/5-LOX inhibitors, Eur. J. Med. Chem. 189 (2020), 112066.

[51] LeadIT, BioSolveIT GmbH, Sankt Augustin, Germany, 2017. http://www.biosolveit.de/LeadIT/.